

# Translational Invariance and Classification of Entanglement in Multipartite States

H. T. Cui(崔海涛),\* and J. L. Tian(田俊龙), C. M. Wang(王春明), Y. C. Chen(陈永超)  
*School of Physics and Electric Engineering, Anyang Normal University, Anyang 455000, China*  
 (Dated: December 3, 2024)

A complete classification of entangled states in  $N$ -qubit systems is constructed, by imposing translational invariance. The symmetric basis is founded, which could be divided into several distinct phases by two global features, periodic pattern and cyclic unit. An understanding of equivalence of entangled states is constructed from phase transition point; The inequivalent entangled states must belong to different phases, and the transformation between them inevitably is accompanied with phase transition. In addition a state composed by different phases is classified as the symmetry-broken phase since it includes distinct global features.

PACS numbers: 03.65.Ud; 03.67.Mn

There are two fundamental issues for a given multipartite entangled state, which one has to identify in order to distinguish one from others, the pattern of entangled state and the measurement of entanglement. Since the construction of GHZ and W states of three qubit [1], it becomes an active area how to present a general classification of multipartite entangled states by stochastic local operations and classical communication (SLOCC). However this task is far from completion. Even for the simple 4-qubit entangled states, there are some inconsistent classifications, based on different prerequisites [2–4]. The difficulty is from the fact that the entanglement in multipartite states is global and the local measurements cannot present the full information of entanglement. Although this difficulty, some methods have been proposed for classification of multipartite entangled states, focused on different aspects. A natural candidate is the generalization of Schmit decomposition into multipartite case [5]. Furthermore the so-called Schmit tensor rank has also been introduced, of which the crucial idea is to find the minimal decomposition on the product basis [6]. Another method is to find the polynomial invariants under SLOCC, of which the distinct pattern can be used to classify the multipartite entanglement [3, 7]. Besides these works, there are distributed efforts focus on other characters of multipartite entanglement, such as the generalized majorization [8], criteria of inequality [9], local unitary equivalence [10], graphical methods [11], and the relaxations [12].

A common point for the previous studies is the general interest in the local features of multipartite entangled states. Recently the global symmetry of multipartite entangled states has received extensive attention [13–15]. Especially a classification of permutation-invariant multipartite entangled states has been obtained by identifying the substructure in entangled states [14] or finding the roots of a Majorana polynomial [15]. It is expected that the overall feature of entangled state could be manifested from global viewpoints. Thus it is possible to construct a complete classification of multipartite entanglement by imposing some global symmetry on multipartite states.

In this letter, a classification of multipartite entangled state is proposed, based on a symmetric basis with translational invariance. Our study shows that for arbitrary  $N$ -qubit system, the symmetric basis can be divided into several topologically distinct classes by two global features of state. Furthermore the concept of *phase* can be also defined from topologically distinct characters. We argue that the conversion between different phases has to accompany with *phase transition*. Furthermore arbitrary state, which is the superposition of the basis states, is considered as symmetry-broken since it would display at least two distinct global features at the same time. Then these superposition states are all classified as a single phase, symmetry-broken phase. Thus A complete classification of entangled states in  $N$ -qubit system can be constructed.

*Symmetry of state* is defined as

**Definition 1** For a symmetry operator  $\hat{S}$ , if

$$\hat{S}|\psi\rangle = c|\psi\rangle, \quad (1)$$

then  $|\psi\rangle$  is said to be with symmetry  $S$  or invariant under  $\hat{S}$ .

The constant  $c$  is complex with unit norm, as shown in Appendix.  $|\psi\rangle$ 's with different  $c$  are obviously orthogonal to each other since Eq. (1) is an eigen equation of operator  $\hat{S}$ . Thus the basis of space can be composed from the eigenvectors of  $\hat{S}$ .

Symmetry of state manifests the global feature of state. Thus by this feature distinct multipartite entangled state can be identified. A crucial question is what symmetry is suitable for this purpose? Our answer is translational invariance, including permutational invariance as a special case. The reason comes from the formal understanding of entanglement; Entanglement actually describes the coherent correlation of single-party states belong to distinguished parties. Suppose every single-party state as a lattice site. Then one has a lattice model for  $N$ -qubit system, composed of two  $N$ -site sublattices as shown in Fig.3 in Appendix. A qubit is represented by two sites belong

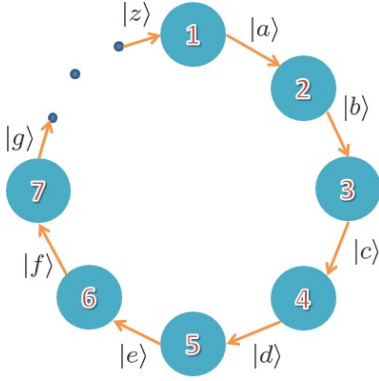


FIG. 1: (Color online) Diagram of the translational operation  $\hat{T}$  of  $N$ -qubit states. The bra vectors denote single-party state, and arabic numbers denote distinct qubits. Then  $\hat{T}$  corresponds to the clock-wise rotation of all single-party states.

to different sublattices with same labels. Then the entangled state up to superposition coefficients can be represented by the lines, which connect the lattice sites with distinct labels. As for this lattice model, translational invariance is much fundamental. In addition the periodic boundary condition (PBC) is supposed automatically.

With this picture, translational operation  $\hat{T}$  is defined schematically in Fig.1, in which PBC of  $N$ -qubit state displays  $|\psi\rangle_{N+i} = |\psi\rangle_i$  for single-party state  $|\psi\rangle_i$ . It should emphasize that  $\hat{T}$  is implemented only for single-party states, not for concrete particles in contrast to that in solid physics.

*Construction of symmetric basis of  $N$ -qubit system*  
The first task is to find the possible values of  $c$  in Eq.(1). By several examples in Appendix, one obtains the conclusion,

**Observation 1** For  $N$ -qubit state, the eigenvalues  $c$  of translational operation  $\hat{T}$  equal to  $\frac{2n\pi}{N}$  with  $n = 0, 1, 2, \dots, N-1$ .

This observation is not strange since the translational operation  $\hat{T}$ , defined in Fig.1, actually displays a cyclic rotation of all single-party states. Thus  $\hat{T}$  behaviors a planar rotation  $C_N$ , and the values of  $c$  correspond to the characters of point group  $C_N$  [16].

In order to construct the symmetric basis of  $N$ -qubit system, it is necessary to impose some restrictions on the construction of basis states. The restrictions are that the cyclic unit should be unique, and its structure should be elementary. As exemplifications, we present the symmetric bases for  $N = 3, 4, 5, 6$  cases in Appendix. It is obvious, for instance that the uniquely cyclic unit in  $|W_1\rangle_3$  is three single-party states,  $|1\rangle, |0\rangle$  and  $|0\rangle$ . In contrast the cyclic unit in  $|W_3\rangle_4$  is the ordered four single-party states,  $|1\rangle, |1\rangle, |0\rangle$  and  $|0\rangle$ . The common feature of these two basis states are uniqueness of cyclic units, 100 and 1100 respectively, and simplicity in which the single-party states are eigenstates of Pauli operator  $\sigma^z$ . The

choice of cyclic unit is not unique since one could impose arbitrarily a unitary operation. The importance is the uniqueness and simplicity of cyclic unit.

It should emphasize that the relative position of single-party states is crucial. For example the information in the cyclic unit of  $|W_3\rangle_4$  is that there are two nearest neighbored parties having the same state  $|1\rangle$ , the other two having another state  $|0\rangle$ . While, the cyclic unit of  $|GHZ'_1\rangle_4$  provides the information that the next nearest neighbored single-party state always is same, but the nearest neighbored parties have different states. This distinct cyclic units attribute to different global feature of  $|W_3\rangle_4$  and  $|GHZ'_1\rangle_4$ , and can be used as the possible criterion of classification of multipartite states. Similar analysis can be implemented for other states.

A common point for  $N$ -qubit symmetric basis is that there two types of permutational invariant states  $|GHZ_{1(2)}\rangle_N$  and  $|W_{1(2)}\rangle_N$ , which are the generalizations of GHZ and  $W$  states of 3-qubit into  $N$ -qubit case. Some special attention should be paid to  $|W_{1(2)}\rangle_N$ . We argue that it is translational invariant, rather than permutational. This point can be manifested by imposing phase difference between the component items, as exemplification of  $|T_{1(2)}\rangle_3$ , which however does not appear for  $|GHZ_{1(2)}\rangle_N$ . This coincide could attribute to the special cyclic unit of  $|W_{1(2)}\rangle_N$ , in which only one single-party state is  $|1(0)\rangle$ .

The symmetric basis for  $N = 3, 4, 5, 6$ -qubit systems have been presented in Appendix. For qubit systems, the construction is much simple since there are only two single-party state  $|1\rangle$  and  $|0\rangle$ . The only interest is what the number of single-party states  $|1\rangle$  or  $|0\rangle$  is in the cyclic unit and their relative position. Then a translational invariant state is composed of all possible forms of the cyclic unit after rotation depicted in Fig.1. Furthermore the phase difference of cyclic rotation is also important since it leads to different  $c$ .

Finally it should point out that the symmetric basis is not unique since the degenerate eigenstates with  $c$ . However the structure of basis state is unique by the previous restrictions. Consequently the basis state can be represented graphically as the connection of lattice sites in a double lattice model. Furthermore the eigenvalue  $c$  corresponds to the character values of planar rotation group  $C_N$ . In a word, the symmetric basis has clear physical significance, and is the genuine demonstration of space structure in  $N$ -qubit systems.

*Classification of symmetric basis states* The distinguishability of basis states can be realized readily by identifying  $c$  and cyclic unit. While  $c$  presents only the information of phase difference, the cyclic unit is a distinct character of a basis state from the others. From point of SLOCC, this difference is inevitably unlocal since the difference of cyclic units is spread over all qubit because of translation invariance, and can be used as a criterion of SLOCC inequivalence.

Besides the periodic pattern of basis state is also fundamental. For instance there are two types of symmetric states for 4-qubit case, so called 2-period, 4-period, as shown in Appendix; It is obvious that there are two items in  $|\text{GHZ}_{1(2)}\rangle_4$  since the cyclic unit is a double of the string 10, while there are four items in  $|W_{1(2)}\rangle_4$  since the cyclic unit has no repeated substructure as the former. It should point out that this realization is consistent with the idea of Schmit tensor rank, by which two SLOCC-equivalent states show the same tensor rank [6]. As for basis state, the decomposition is minimal since any extra item or absence of any item would destroy translational invariance. Thus  $n$ , the number of items in basis state decomposition, is also a global feature of basis state, which is called  $n$ -period in this place. An exceptional case is  $|\text{GHZ}_{1(2)}\rangle_N$ , which is defined forcibly as 1-period only for completion. It should point out that this definition does not mean that the periodic pattern of  $|\text{GHZ}_{1(2)}\rangle_N$  is distinguished since one can find for example that  $|\text{GHZ}_{1(2)}\rangle_4$  and  $|\text{GHZ}'_{1(2)}\rangle_4$  can be converted each other by LOCC, as shown in Appendix.

A crucial observation is

**Observation 2** *For  $N = n \times m$  qubit system, there exist  $n$ -period or  $m$ -period translation invariant basis state, besides of the trivial cases 1-period.*

This result can be understood from the point of group theory; For  $N = n \times m$ , one has decomposition  $C_N = C_n \otimes C_m$ . That is to say that the point group  $C_N$  is the direct product of subgroups  $C_n$  and  $C_m$ . For example,  $C_4 = C_2 \otimes C_2$ ,  $C_6 = C_2 \otimes C_3$  [16]. As for symmetric basis states, this decomposition means that there are different translation structures, labeled by the periodic pattern of basis state.

Totally one can classify the basis states by two global features, *periodic pattern* and *cyclic unit*. The periodic pattern provides the geometrical property of Hilbert space; Observation 2 is just the illustration of symmetric structures embedded in  $N$ -qubit space. These structures obviously cannot be changed by any local invertible operation, and can be used to differentiate different basis states. While, the cyclic unit presents the details of states. In general, there may be different cyclic units for a certain periodic pattern, as shown in Appendix. However it does not mean that the state with different cyclic units can be converted into each other by SLOCC since the difference of cyclic units is spread over all qubit because of translation invariance.

*Phase transition point of the classification of symmetric basis states* Mathematically SLOCC corresponds to continuous transformation since its local feature and invertibility. Thus two SLOCC-inequivalent states must have different characters such that one cannot transform one continuously into another; Geometrically these characters are inevitably global or topological. By imposing

certain symmetry, these distinct characters can be readily identified by distinct structures of symmetry.

Consequently one can identify a periodic pattern as a *phase* from theory of phase transition. Thus the conversion of different phases have to be accompanied with *phase transition*, which corresponds to a singular behavior. In addition a phase is also topological from the point that there are generally distinct cyclic units; The degeneracy is sometime robust since its breaking has to introduce the long-range interaction, as shown in the final part of Appendix. Furthermore one can define *quantum number* to label different phases. In this letter these quantum numbers are just the common divisors of qubit number  $N$  by Observation 2, except of the trivial 1-period case.

A special case is about states  $|\text{GHZ}_{1(2)}\rangle_N$  and  $|\text{GHZ}'_{1(2)}\rangle_N$  for even  $N$ , which are obviously LOCC equivalent. Thus they are classified as the same one, although  $|\text{GHZ}_{1(2)}\rangle_N$  is permutational invariant, not for  $|\text{GHZ}'_{1(2)}\rangle_N$ . This situation shows that permutational invariance is not a intrinsic feature of state; Any state with permutational invariance can be decomposed as the superposition of symmetric basis states, for example, the Dicke state

$$\begin{aligned} |S(4;2)\rangle &= \frac{1}{\sqrt{6}} \sum_{\text{permutation}} |1100\rangle \\ &= \sqrt{\frac{4}{3}} |W_2\rangle_4 + \sqrt{\frac{1}{3}} |\text{GHZ}'_1\rangle_4 \end{aligned} \quad (2)$$

*Generalization to arbitrary states* Two situations can be identified. One is when a multipartite state is fully separable, i.e.  $|\psi\rangle = \otimes_{n=1}^N |\varphi_n\rangle$ . It is known that all fully separable states are LOCC-equivalent via local unitary operation  $U = \otimes_{n=1}^N u_n$ . The fully separable states can be classified as the *classical* phase since there is no any entanglement.

The other case is for a general entangled state, which can be decomposed under the symmetric basis. Since it is composed of different global entanglements, we call it *hybrid*. An important observation is for symmetric basis states,

**Observation 3** *For a definite cyclic unit, there is no degeneracy for  $c$ ; For degenerate  $c$ , the degenerate states correspond to distinct cyclic units respectively.*

Then two cases can be founded; One is for the hybrid state which is the superposition of the basis states with different  $c$ . Thus the translational invariance is inevitably broken in this situation. The other is for the hybrid state which is the superposition of the basis states with the same  $c$ . Although the translational invariance would be preserved, the state may include different periodic patterns or cyclic units. Then the global symmetry is also broken.

Thus all hybrid states can be classified as the *symmetry-broken* phase. This conclusion is similar to

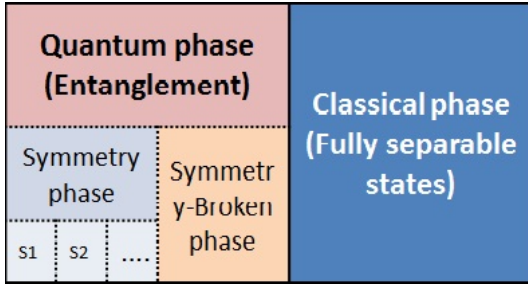


FIG. 2: (Color online) A complete phase diagram for  $N$ -qubit states. The labels  $S1, S2, \dots$  denotes the different symmetric entangled states, differentiated by the periodic pattern and cyclic unit.

that for a classification of gapped symmetric ground states in one-dimensional spin systems [17]; An interesting result in this work is that all gapped one-dimensional ground states belong to the same phase if there is no symmetry. With respect that the symmetry could include the global features, such as periodic pattern and cyclic unit, the state composed of the distinct global features is breaking topological symmetry.

*Discussion and Conclusion* A complete phase diagram is constructed, as shown in Fig.2. By the property of entanglement, two grand classes can be identified as classical phase and quantum phase. It should emphasize that the term of quantum phase is used to emphasize the difference between entangled and fully separable state in this place, indifferent to the definition in condensed matter phase [18]. As for quantum phase, there are two subclasses. When translational invariance is imposed, a symmetric basis can be constructed, which is divided into several classes by periodic pattern and cyclic unit. Whenever there is no symmetry, all states are classified as symmetry-broken phase. We have to admit that it is coarse since there are some interesting situations to identify case by case. Actually hybrid state could be considered as a intermediated state from the point of dynamics of phase transition. Thus its behavior is dependent on concrete Hamiltonian.

In conclusion, a complete classification of  $N$ -qubit entangled states is presented in this article, based on the concept of phase transition. By imposing the translational invariance, the symmetric basis can be constructed readily, which is the manifestation of the global features of entangled states. By identifying periodic pattern and cyclic unit, the symmetric basis states can be divided into several inequivalent classes. We wish this discussion would be helpful for the general understanding of multipartite entanglement.

HTC acknowledges the fruitful discussion with Dr. Chang-Shui Yu. This work is supported by NSF of China, Grant No. 11005002 and 11005003, and Sponsorship Program of Excellent Younger Teachers of University in Henan Province, Grant No. 2010GGJS-181.

\* Electronic address: cuiht@aynu.edu.cn

- [1] W. Dür, G. Vidal and J. I. Cirac, Phys. Rev. A **62**, 062314 (2000).
- [2] F. Verstraete, J. Dehaene, B. De Moor, and H. Verschelde, Phys. Rev. A **65**, 052112 (2002).
- [3] A. Osterloh, and J. Siewert, Phys. Rev. A **72**, 012337 (2005).
- [4] L. Lamata, J. Léon, D. Salgado, and E. Solano, Phys. Rev. A, **74**, 052336 (2006); **75**, 022318 (2007); Y. Cao, and A. M. Wang, Eur. Phys. J. D **44**, 159 (2007); E. Chitambar, R. Duan, and Y. Shi, Phys. Rev. Lett. **101**, 140502 (2008); D. Li, X. Li, H. Huang, and X. Li, Quant. Info. Comp. **9**, 0778 (2009); L. borsten, d. Dahanayake, M. J. Duff, A. Marrani, and W. Rubens, Phys. Rev. Lett. **105**, 100507 (2010); G. Gour, and N. R. Wallach, J. Math. Phys. **51**, 112201 (2010).
- [5] A. Acín, A. Andrianov, L. Casta, E. Jané, J. I. Latorre, and R. Tarrach, Phys. Rev. Lett. **85**, 1560 (2000); H. A. Carteret, H. Higuchi, and A. Sudbery, J. Math. Phys. **41**, 7932 (2000); L. Lamata, J. León, D. Salgado, and E. Solano, Phys. Rev. A **74**, 052336 (2006); **75**, 022318 (2007).
- [6] E. Chitambar, R. Duan, and Y. Shi, Phys. Rev. Lett. **101**, 140502 (2008); R. Duan, and Y. Shi, e-print at arXiv: 0911.0879[quant-ph]; L. Chen, E. Chitambar, R. Duan, Z. Ji, and A. Winter, Phys. Rev. Lett. **105**, 200501 (2010); L. Chen, and M. Hayashi, Phys. Rev. A **82**, 022331 (2011).
- [7] M. Grassl, M. Rötteler, and T. Beth, Phys. Rev. A **58**, 1833 (1998); A. Miyake, *ibid*, **67**, 012108 (2003); M. S. Leifer, N. Linden, and A. Winter, *ibid*, **69**, 052304 (2004); D. Ž. Doković, and A. Osterloh, J. Math. Phys. **50**, 033509 (2009); O. Viehmann, C. Eltschka, and J. Siewert, e-print at arXiv: 1101.5558[quant-ph].
- [8] G. Gour, and N. R. Wallach, e-print at arXiv:1103.5096[quant-ph].
- [9] C. Schmid, N. Kiesel, W. Lashkowski, W. Wiczkorek, M. Żukowski, and H. Weinfurter, Phys. Rev. Lett. **100**, 200407 (2008); M. Huber, F. Mintert, A. Gabriel, and B. C. Hiesmayr, *ibid*, **104**, 210501 (2010).
- [10] B. Kraus, Phys. Rev. Lett. **104**, 020504 (2010); Phys. Rev. A **82**, 032121 (2010); A. Sawicki, and M. Kuś, e-print at arXiv:1009.0293v1 [quant-ph].
- [11] M. S. Williamson, M. Ericsson, M. Johansson, E. Sjöqvist, A. Sudbery, V. Vedral, and William K. Wootters, e-print at arXiv:1102.4222v1 [quant-ph].
- [12] B. Jungnitsch, T. Moroder, and O. Gühne, Phys. Rev. Lett. **106**, 190502 (2011).
- [13] M. Huber, N. Friis, A. Gabriel, C. Spengler, and B. C. Hiesmayr, e-print at arXiv:1011.3374v1 [quant-ph]; I. Marvian, and R. W. Spekkens, e-print at arXiv:1105.1816 [quant-ph]; D. W. Lyons, and S. N. Walck, e-print at arXiv:1107.1372 [quant-ph].
- [14] T. Bastin, S. Krins, P. Mathonet, M. Godefroid, L. Lamata, E. Solano, Phys. Rev. Lett. **103**, 070503 (2009); P. Mathonet, S. Krins, M. Godefroid, L. Lamata, E. Solano, T. Bastin, Phys. Rev. A **81**, 052315 (2010);
- [15] P. Ribeiro, and R. Mosseri, Phys. Rev. Lett. **106**, 180502 (2011); M. Aulbach, e-print at arXiv:1103.0271v2 [quant-ph]; A.R. Usha Devi, Sudha, and A. K. Rajagopal, e-print at arXiv:1103.3640v1 [quant-ph]; D. J.

- H. Markham, Phys. Rev. A **83**, 042332 (2011).
- [16] J. F. Cornwell, *Group Theory in Physics: an Introduction*, Academic Press (1997).
- [17] X. Chen, Z.-C. Gu, and X.-G. Wen, Phys. Rev. B, **83**, 035107 (2011).
- [18] X.-G. Wen, Adv. Phys. **44**, 405 (1995).

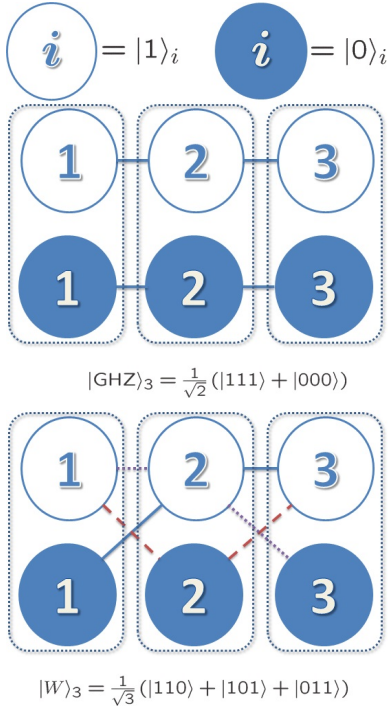


FIG. 3: (Color online) A graphical representation of 3-qubit entangled states.

### Graphic representation of entangled state

For a qubit there two orthogonal states  $|1\rangle$  and  $|0\rangle$ . One then can conjecture that a qubit could be composed from two pseudo particles, as shown in Fig.3. This picture comes from the understanding of entanglement that actually defines the connection between single-party states belong to different qubits, up to superposition coefficients. As a example, Fig.3 provides graphic representations of  $|\text{GHZ}\rangle_3$  and  $|W\rangle$ . The scheme can be generalized readily to arbitrary  $N$ -qubit state.

The obvious defect of this method is that it cannot manifest the different superposition coefficients. Furthermore the graph would become complicated for large  $N$ . However it is unimportant since the purpose of this section is to provide the intuition of  $N$ -qubit system by a lattice model with two sublattices. Then the entanglement of qubits is actually the connection of lattice site with different label  $i$ .

### Several examples of the construction of symmetric basis

This section provides several examples for an illustration of Observation 1.

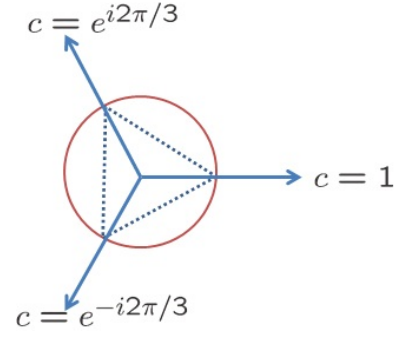


FIG. 4: (Color online) A graphical illustration of the value of  $c$  in Eq.(1) for 3-qubit case.

### 3-qubit case

The symmetric basis is

$$\begin{aligned}
 |\text{GHZ}_1\rangle_3 &= \frac{1}{\sqrt{2}} (|111\rangle + |000\rangle) \\
 |\text{GHZ}_2\rangle_3 &= \frac{1}{\sqrt{2}} (|111\rangle - |000\rangle) \\
 |W_1\rangle_3 &= \frac{1}{\sqrt{3}} (|100\rangle + |010\rangle + |001\rangle) \\
 |W_2\rangle_3 &= \frac{1}{\sqrt{3}} (|110\rangle + |011\rangle + |101\rangle) \\
 |T_1\rangle_3 &= \frac{1}{\sqrt{3}} (|100\rangle + e^{i2\pi/3}|010\rangle + e^{i4\pi/3}|001\rangle) \\
 |T_1^*\rangle_3 &= (|T_1\rangle_3)^* \\
 |T_2\rangle_3 &= \frac{1}{\sqrt{3}} (|110\rangle + e^{i2\pi/3}|101\rangle + e^{i4\pi/3}|011\rangle) \\
 |T_2^*\rangle_3 &= (|T_2\rangle_3)^*, \tag{3}
 \end{aligned}$$

Besides of  $|\text{GHZ}_{1(2)}\rangle_3$  and  $|W_{1(2)}\rangle_3$ , it is easy to show

$$\begin{aligned}
 \hat{T}|T_1\rangle_3 &= \frac{1}{\sqrt{3}} (|010\rangle + e^{i2\pi/3}|001\rangle + e^{i4\pi/3}|100\rangle) \\
 &= e^{-i2\pi/3} \frac{1}{\sqrt{3}} (|100\rangle + e^{i2\pi/3}|010\rangle + e^{i4\pi/3}|001\rangle) \\
 &= e^{-i2\pi/3} |T_1\rangle_3 \tag{4}
 \end{aligned}$$

$$\begin{aligned}
 \hat{T}|T_2\rangle_3 &= \frac{1}{\sqrt{3}} (|011\rangle + e^{i2\pi/3}|110\rangle + e^{i4\pi/3}|101\rangle) \\
 &= e^{i2\pi/3} \frac{1}{\sqrt{3}} (|110\rangle + e^{-i2\pi/3}|011\rangle + e^{i2\pi/3}|101\rangle) \\
 &= e^{i2\pi/3} \frac{1}{\sqrt{3}} (|110\rangle + e^{i4\pi/3}|011\rangle + e^{i2\pi/3}|101\rangle) \\
 &= e^{i2\pi/3} |T_2\rangle_3 \tag{5}
 \end{aligned}$$

Thus  $c = 1, e^{\pm i2\pi/3}$ , and the orthogonal relation of basis states can be easily found by  $1 + e^{i2\pi/3} + e^{i4\pi/3} = 0$ . Interestingly the values of  $c$  corresponds to the characters of point group  $C_3$ , as shown in Fig.4. This feature is popular, as shown in the following subsections.

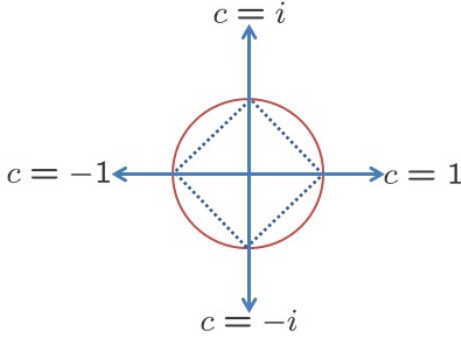


FIG. 5: (Color online) A graphical illustration of the value of  $c$  for 4-qubit case.

It is obvious

$$|T_1\rangle_3 = I \otimes \begin{pmatrix} e^{i2\pi/3} & 0 \\ 0 & 1 \end{pmatrix} \otimes \begin{pmatrix} e^{i4\pi/3} & 0 \\ 0 & 1 \end{pmatrix} |W_1\rangle_3. \quad (6)$$

Similar relation can be found for  $|T_2\rangle_3$ . Thus by LOCC there are two inequivalent classes  $\{|\text{GHZ}_1\rangle_3, |\text{GHZ}_2\rangle_3\}$  and  $\{|W_{1(2)}\rangle_3, |T_{1(2)}\rangle_3, |T_{1(2)}^*\rangle_3\}$ .

#### 4-qubit case

The symmetric basis is

$$|\text{GHZ}_1\rangle_4 = \frac{1}{\sqrt{2}} (|1111\rangle + |0000\rangle)$$

$$|\text{GHZ}_2\rangle_4 = \frac{1}{\sqrt{2}} (|1111\rangle - |0000\rangle)$$

2-period:

$$|\text{GHZ}'_1\rangle_4 = \frac{1}{\sqrt{2}} (|1010\rangle + |0101\rangle)$$

$$|\text{GHZ}'_2\rangle_4 = \frac{1}{\sqrt{2}} (|1010\rangle - |0101\rangle)$$

4-period:

$$|W_1\rangle_4 = \frac{1}{2} (|1000\rangle + |0100\rangle + |0010\rangle + |0001\rangle)$$

$$|T_1\rangle_4 = \frac{1}{2} (|1000\rangle + e^{i\pi/2}|0100\rangle + e^{i\pi}|0010\rangle + e^{i3\pi/2}|0001\rangle)$$

$$|T_1^*\rangle_4 = (|T_1\rangle_4)^*$$

$$|T_1'\rangle_4 = \frac{1}{2} (|1000\rangle - |0100\rangle + |0010\rangle - |0001\rangle)$$

$$|W_2\rangle_4 = \frac{1}{2} (|1110\rangle + |1101\rangle + |1011\rangle + |0111\rangle)$$

$$|T_2\rangle_4 = \frac{1}{2} (|1110\rangle + e^{i\pi/2}|1101\rangle + e^{i\pi}|1011\rangle + e^{i3\pi/2}|0111\rangle)$$

$$|T_2^*\rangle_4 = (|T_2\rangle_4)^*$$

$$|T_2'\rangle_4 = \frac{1}{2} (|1110\rangle - |1101\rangle + |1011\rangle - |0111\rangle)$$

$$\begin{aligned} |W_3\rangle_4 &= \frac{1}{2} (|1100\rangle + |0110\rangle + |0011\rangle + |1001\rangle) \\ |T_3\rangle_4 &= \frac{1}{2} (|1100\rangle + e^{i\pi/2}|0110\rangle + e^{i\pi}|0011\rangle + e^{i3\pi/2}|1001\rangle) \\ |T_3^*\rangle_4 &= (|T_3\rangle_4)^* \\ |T_3'\rangle_4 &= \frac{1}{2} (|1100\rangle - |0110\rangle + |0011\rangle - |1001\rangle) \end{aligned} \quad (7)$$

Besides of  $|\text{GHZ}_{1(2)}\rangle_4$  and  $|W_{1(2,3)}\rangle_4$ , it is ready to verify

$$\begin{aligned} \hat{T}|\text{GHZ}'_1\rangle_4 &= |\text{GHZ}'_1\rangle_4 \\ \hat{T}|\text{GHZ}'_2\rangle_4 &= -|\text{GHZ}'_2\rangle_4 \\ \hat{T}|T_1\rangle_4 &= -i|T_1\rangle_4 \\ \hat{T}|T_2\rangle_4 &= i|T_2\rangle_4 \\ \hat{T}|T_3\rangle_4 &= -i|T_3\rangle_4 \\ \hat{T}|T'_{1(2,3)}\rangle_4 &= -|T'_{1(2,3)}\rangle_4. \end{aligned} \quad (8)$$

Thus  $c = \pm 1, \pm i$ , which are the characters of point group  $C_4$  as shown in Fig.5.

Obviously one has LOCC equivalences

$$\begin{aligned} |T_1\rangle_4 &= I \otimes \begin{pmatrix} e^{i\pi/2} & 0 \\ 0 & 1 \end{pmatrix} \otimes \begin{pmatrix} e^{i\pi} & 0 \\ 0 & 1 \end{pmatrix} \otimes \begin{pmatrix} e^{i3\pi/2} & 0 \\ 0 & 1 \end{pmatrix} |W_1\rangle_4 \\ |T_1'\rangle_4 &= I \otimes \begin{pmatrix} -1 & 0 \\ 0 & 1 \end{pmatrix} \otimes I \otimes \begin{pmatrix} -1 & 0 \\ 0 & 1 \end{pmatrix} |W_1\rangle_4 \\ |T_3\rangle_4 &= I \otimes \begin{pmatrix} e^{i\pi/2} & 0 \\ 0 & 1 \end{pmatrix} \otimes \begin{pmatrix} e^{i\pi} & 0 \\ 0 & 1 \end{pmatrix} \otimes \begin{pmatrix} e^{i3\pi/2} & 0 \\ 0 & 1 \end{pmatrix} |W_3\rangle_4 \\ |T_3'\rangle_4 &= I \otimes \begin{pmatrix} -1 & 0 \\ 0 & 1 \end{pmatrix} \otimes I \otimes \begin{pmatrix} -1 & 0 \\ 0 & 1 \end{pmatrix} |W_3\rangle_4 \end{aligned} \quad (9)$$

With respect to distinct cyclic units in  $|W_3\rangle_4$  to those in  $|W_3\rangle_{1(2)}$ , there are three LOCC inequivalent classes,  $\{|\text{GHZ}_{1(2)}\rangle_4, |\text{GHZ}'_{1(2)}\rangle_4\}$ ,  $\{|W_{1(2)}\rangle_4, |T_{1(2)}\rangle_4, |T_{1(2)}^*\rangle_4, |T'_{1(2)}\rangle_4\}$  and  $\{|W_3\rangle_4, |T_3\rangle_4, |T_3^*\rangle_4, |T_3'\rangle_4\}$ .

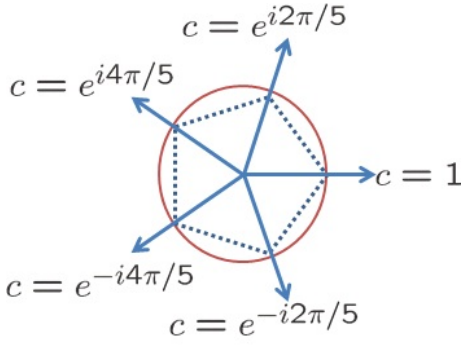


FIG. 6: (Color online) A graphical illustration of the value of  $c$  in Eq.(1) for 5-qubit case.

### 5-qubit case

The symmetric basis is

$$\begin{aligned}
 |\text{GHZ}_1\rangle_5 &= \frac{1}{\sqrt{2}} (|11111\rangle + |00000\rangle) \\
 |\text{GHZ}_2\rangle_5 &= \frac{1}{\sqrt{2}} (|11111\rangle - |00000\rangle) \\
 |W_1\rangle_5 &= \frac{1}{\sqrt{5}} (|10000\rangle + |01000\rangle + |00100\rangle \\
 &\quad + |00010\rangle + |00001\rangle) \\
 |T_1\rangle_5 &= \frac{1}{\sqrt{5}} (|10000\rangle + e^{i2\pi/5}|01000\rangle + e^{i4\pi/5}|00100\rangle \\
 &\quad + e^{i6\pi/5}|00010\rangle + e^{i8\pi/5}|00001\rangle) \\
 |T_1^*\rangle_5 &= (|T_1\rangle_5)^* \\
 |T_1'\rangle_5 &= \frac{1}{\sqrt{5}} (|10000\rangle + e^{i4\pi/5}|01000\rangle + e^{i8\pi/5}|00100\rangle \\
 &\quad + e^{i12\pi/5}|00010\rangle + e^{i16\pi/5}|00001\rangle) \\
 |T_1'^*\rangle_5 &= (|T_1'\rangle_5)^* \\
 |W_2\rangle_5 &= \frac{1}{\sqrt{5}} (|01111\rangle + |10111\rangle + |11011\rangle \\
 &\quad + |11101\rangle + |11110\rangle) \\
 |T_2\rangle_5 &= \frac{1}{\sqrt{5}} (|01111\rangle + e^{i2\pi/5}|10111\rangle + e^{i4\pi/5}|11011\rangle \\
 &\quad + e^{i6\pi/5}|11101\rangle + e^{i8\pi/5}|11110\rangle) \\
 |T_2^*\rangle_5 &= (|T_2\rangle_5)^* \\
 |T_2'\rangle_5 &= \frac{1}{\sqrt{5}} (|01111\rangle + e^{i4\pi/5}|10111\rangle + e^{i8\pi/5}|11011\rangle \\
 &\quad + e^{i12\pi/5}|11101\rangle + e^{i16\pi/5}|11110\rangle) \\
 |T_2'^*\rangle_5 &= (|T_2'\rangle_5)^* \\
 |W_3\rangle_5 &= \frac{1}{\sqrt{5}} (|11000\rangle + |01100\rangle + |00110\rangle + \\
 &\quad |00011\rangle + |10001\rangle)
 \end{aligned}$$

$$\begin{aligned}
 |T_3\rangle_5 &= \frac{1}{\sqrt{5}} (|11000\rangle + e^{i2\pi/5}|01100\rangle + e^{i4\pi/5}|00110\rangle \\
 &\quad + e^{i6\pi/5}|00011\rangle + e^{i8\pi/5}|10001\rangle) \\
 |T_3^*\rangle_5 &= (|T_3\rangle_5)^* \\
 |T_3'\rangle_5 &= \frac{1}{\sqrt{5}} (|11000\rangle + e^{i4\pi/5}|01100\rangle + e^{i8\pi/5}|00110\rangle \\
 &\quad + e^{i12\pi/5}|00011\rangle + e^{i16\pi/5}|10001\rangle) \\
 |T_3'^*\rangle_5 &= (|T_3'\rangle_5)^* \\
 |W_4\rangle_5 &= \frac{1}{\sqrt{5}} (|00111\rangle + |10011\rangle + |11001\rangle \\
 &\quad + |11100\rangle + |01110\rangle) \\
 |T_4\rangle_5 &= \frac{1}{\sqrt{5}} (|00111\rangle + e^{i2\pi/5}|10011\rangle + e^{i4\pi/5}|11001\rangle \\
 &\quad + e^{i6\pi/5}|11100\rangle + e^{i8\pi/5}|01110\rangle) \\
 |T_4^*\rangle_5 &= (|T_4\rangle_5)^* \\
 |T_4'\rangle_5 &= \frac{1}{\sqrt{5}} (|00111\rangle + e^{i4\pi/5}|10011\rangle + e^{i8\pi/5}|11001\rangle \\
 &\quad + e^{i12\pi/5}|11100\rangle + e^{i16\pi/5}|01110\rangle) \\
 |T_4'^*\rangle_5 &= (|T_4'\rangle_5)^* \\
 |W_5\rangle_5 &= \frac{1}{\sqrt{5}} (|10100\rangle + |01010\rangle + |00101\rangle + \\
 &\quad |10010\rangle + |01001\rangle) \\
 |T_5\rangle_5 &= \frac{1}{\sqrt{5}} (|10100\rangle + e^{i2\pi/5}|01010\rangle + e^{i4\pi/5}|00101\rangle + \\
 &\quad e^{i6\pi/5}|10010\rangle + e^{i8\pi/5}|01001\rangle) \\
 |T_5^*\rangle_5 &= (|T_5\rangle_5)^* \\
 |T_5'\rangle_5 &= \frac{1}{\sqrt{5}} (|10100\rangle + e^{i4\pi/5}|01010\rangle + e^{i8\pi/5}|00101\rangle + \\
 &\quad e^{i12\pi/5}|10010\rangle + e^{i16\pi/5}|01001\rangle) \\
 |T_5'^*\rangle_5 &= (|T_5'\rangle_5)^* \\
 |W_6\rangle_5 &= \frac{1}{\sqrt{5}} (|01011\rangle + |10101\rangle + |11010\rangle + \\
 &\quad |01101\rangle + |10110\rangle) \\
 |T_6\rangle_5 &= \frac{1}{\sqrt{5}} (|01011\rangle + e^{i2\pi/5}|10101\rangle + e^{i4\pi/5}|11010\rangle + \\
 &\quad e^{i6\pi/5}|01101\rangle + e^{i8\pi/5}|10110\rangle) \\
 |T_6^*\rangle_5 &= (|T_6\rangle_5)^* \\
 |T_6'\rangle_5 &= \frac{1}{\sqrt{5}} (|01011\rangle + e^{i4\pi/5}|10101\rangle + e^{i8\pi/5}|11010\rangle + \\
 &\quad e^{i12\pi/5}|01101\rangle + e^{i16\pi/5}|10110\rangle) \\
 |T_6'^*\rangle_5 &= (|T_6'\rangle_5)^* .
 \end{aligned} \tag{10}$$

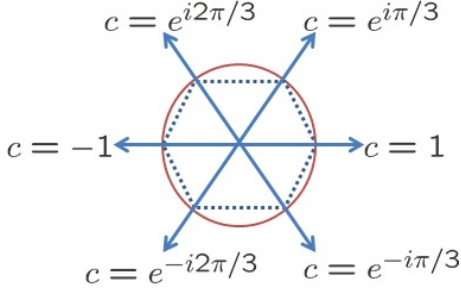


FIG. 7: (Color online) A graphical illustration of the value of  $c$  in Eq.(1) for 6-qubit case.

It is easy to verify, for instance,

$$\begin{aligned}
 \hat{T}|T_1\rangle_5 &= \frac{1}{\sqrt{5}} \left( |01000\rangle + e^{i2\pi/5}|00100\rangle + e^{i4\pi/5}|00010\rangle \right. \\
 &\quad \left. + e^{i6\pi/5}|00001\rangle + e^{i8\pi/5}|10000\rangle \right) \\
 &= \frac{e^{i8\pi/5}}{\sqrt{5}} \left( |10000\rangle + e^{i2\pi/5}|01000\rangle + e^{i4\pi/5}|00100\rangle \right. \\
 &\quad \left. + e^{i6\pi/5}|00010\rangle + e^{i8\pi/5}|00001\rangle \right) \\
 &= e^{-i2\pi/5}|T_1\rangle_5 \\
 \hat{T}|T'_1\rangle_5 &= \frac{1}{\sqrt{5}} \left( |01000\rangle + e^{i4\pi/5}|00100\rangle + e^{i8\pi/5}|00010\rangle \right. \\
 &\quad \left. + e^{i12\pi/5}|00001\rangle + e^{i16\pi/5}|10000\rangle \right) \\
 &= e^{-i4\pi/5}|T'_1\rangle_5.
 \end{aligned} \tag{11}$$

The other values of  $c$  can be also obtained by similar method. Obviously the values of  $c$  are just the characters of point group  $C_5$ , as shown in Fig.6.

There are 4 classes, dependent on the periodicity and the cyclic unit,

$$\begin{aligned}
 &\{|\text{GHZ}_{1(2)}\rangle_5\}, \\
 &\{|W_{1(2)}\rangle_5, |T_{1(2)}\rangle_5, |T_{1(2)}^*\rangle_5, |T'_{1(2)}\rangle_5\}, \\
 &\{|W_{3(4)}\rangle_5, |T_{3(4)}\rangle_5, |T_{3(4)}^*\rangle_5, |T'_{3(4)}\rangle_5\}, \\
 &\{|W_{5(6)}\rangle_5, |T_{5(6)}\rangle_5, |T_{5(6)}^*\rangle_5, |T'_{5(6)}\rangle_5\}
 \end{aligned} \tag{12}$$

### 6-qubit case

The symmetric basis is

$$\begin{aligned}
 |\text{GHZ}_1\rangle_6 &= \frac{1}{\sqrt{2}} (|111111\rangle + |000000\rangle) \\
 |\text{GHZ}_2\rangle_6 &= \frac{1}{\sqrt{2}} (|111111\rangle - |000000\rangle)
 \end{aligned}$$

6-period:

$$\begin{aligned}
 |W_1\rangle_6 &= \frac{1}{\sqrt{6}} (|100000\rangle + |010000\rangle + |001000\rangle \\
 &\quad + |000100\rangle + |000010\rangle + |000001\rangle) \\
 |T_1\rangle_6 &= \frac{1}{\sqrt{6}} \left( |100000\rangle + e^{i\pi/3}|010000\rangle + e^{i2\pi/3}|001000\rangle \right. \\
 &\quad \left. + e^{i\pi}|000100\rangle + e^{i4\pi/3}|000010\rangle + e^{i5\pi/3}|000001\rangle \right) \\
 |T_1^*\rangle_6 &= (|T_1\rangle_6)^* \\
 |T'_1\rangle_6 &= \frac{1}{\sqrt{6}} \left( |100000\rangle + e^{i2\pi/3}|010000\rangle + e^{i4\pi/3}|001000\rangle \right. \\
 &\quad \left. + |000100\rangle + e^{i2\pi/3}|000010\rangle + e^{i4\pi/3}|000001\rangle \right) \\
 |T_1'^*\rangle_6 &= (|T'_1\rangle_6)^* \\
 |T_1''\rangle_6 &= \frac{1}{\sqrt{6}} (|100000\rangle - |010000\rangle + |001000\rangle \\
 &\quad - |000100\rangle + |000010\rangle - |000001\rangle) \\
 |W_2\rangle_6 &= \frac{1}{\sqrt{6}} (|011111\rangle + |101111\rangle + |110111\rangle \\
 &\quad + |111011\rangle + |111101\rangle + |111110\rangle) \\
 |T_2\rangle_6 &= \frac{1}{\sqrt{6}} \left( |011111\rangle + e^{i\pi/3}|101111\rangle + e^{i2\pi/3}|110111\rangle \right. \\
 &\quad \left. + e^{i\pi}|111011\rangle + e^{i4\pi/3}|111101\rangle + e^{i5\pi/3}|111110\rangle \right) \\
 |T_2^*\rangle_6 &= (|T_2\rangle_6)^* \\
 |T'_2\rangle_6 &= \frac{1}{\sqrt{6}} \left( |011111\rangle + e^{i2\pi/3}|101111\rangle + e^{i4\pi/3}|110111\rangle \right. \\
 &\quad \left. + |111011\rangle + e^{i2\pi/3}|111101\rangle + e^{i4\pi/3}|111110\rangle \right) \\
 |T_2'^*\rangle_6 &= (|T'_2\rangle_6)^* \\
 |T_2''\rangle_6 &= \frac{1}{\sqrt{6}} (|011111\rangle - |101111\rangle + |110111\rangle \\
 &\quad - |111011\rangle + |111101\rangle - |111110\rangle) \\
 |W_3\rangle_6 &= \frac{1}{\sqrt{6}} (|110000\rangle + |011000\rangle + |001100\rangle \\
 &\quad + |000110\rangle + |000011\rangle + |100001\rangle) \\
 |T_3\rangle_6 &= \frac{1}{\sqrt{6}} \left( |110000\rangle + e^{i\pi/3}|011000\rangle + e^{i2\pi/3}|001100\rangle \right. \\
 &\quad \left. + e^{i\pi}|000110\rangle + e^{i4\pi/3}|000011\rangle + e^{i5\pi/3}|100001\rangle \right) \\
 |T_3^*\rangle_6 &= (|T_3\rangle_6)^* \\
 |T'_3\rangle_6 &= \frac{1}{\sqrt{6}} \left( |110000\rangle + e^{i2\pi/3}|011000\rangle + e^{i4\pi/3}|001100\rangle \right. \\
 &\quad \left. + |000110\rangle + e^{i2\pi/3}|000011\rangle + e^{i4\pi/3}|100001\rangle \right) \\
 |T_3'^*\rangle_6 &= (|T'_3\rangle_6)^* \\
 |T_3''\rangle_6 &= \frac{1}{\sqrt{6}} (|110000\rangle - |011000\rangle + |001100\rangle \\
 &\quad - |000110\rangle + |000011\rangle - |100001\rangle)
 \end{aligned}$$

$$\begin{aligned}
|W_4\rangle_6 &= \frac{1}{\sqrt{6}} (|001111\rangle + |101111\rangle + |110011\rangle \\
&\quad + |111001\rangle + |111100\rangle + |011110\rangle) \\
|T_4\rangle_6 &= \frac{1}{\sqrt{6}} \left( |001111\rangle + e^{i\pi/3}|100111\rangle + e^{i2\pi/3}|110011\rangle \right. \\
&\quad \left. + e^{i\pi}|111001\rangle + e^{i4\pi/3}|111100\rangle + e^{i5\pi/3}|011110\rangle \right) \\
|T_4^*\rangle_6 &= (|T_4\rangle_6)^* \\
|T_4'\rangle_6 &= \frac{1}{\sqrt{6}} \left( |001111\rangle + e^{i2\pi/3}|100111\rangle + e^{i4\pi/3}|110011\rangle \right. \\
&\quad \left. + |111001\rangle + e^{i2\pi/3}|111100\rangle + e^{i4\pi/3}|011110\rangle \right) \\
|T_4''\rangle_6 &= \frac{1}{\sqrt{6}} (|001111\rangle - |101111\rangle + |110011\rangle \\
&\quad - |111001\rangle + |111100\rangle - |011110\rangle) \\
|W_5\rangle_6 &= \frac{1}{\sqrt{6}} (|101000\rangle + |010100\rangle + |001010\rangle \\
&\quad + |000101\rangle + |100010\rangle + |010001\rangle) \\
|T_5\rangle_6 &= \frac{1}{\sqrt{6}} \left( |101000\rangle + e^{i\pi/3}|010100\rangle + e^{i2\pi/3}|001010\rangle \right. \\
&\quad \left. + e^{i\pi}|000101\rangle + e^{i4\pi/3}|100010\rangle + e^{i5\pi/3}|010001\rangle \right) \\
|T_5^*\rangle_6 &= (|T_5\rangle_6)^* \\
|T_5'\rangle_6 &= \frac{1}{\sqrt{6}} \left( |101000\rangle + e^{i2\pi/3}|010100\rangle + e^{i4\pi/3}|001010\rangle \right. \\
&\quad \left. + |000101\rangle + e^{i2\pi/3}|100010\rangle + e^{i4\pi/3}|010001\rangle \right) \\
|T_5''\rangle_6 &= \frac{1}{\sqrt{6}} (|101000\rangle - |010100\rangle + |001010\rangle \\
&\quad - |000101\rangle + |100010\rangle - |010001\rangle) \\
|W_6\rangle_6 &= \frac{1}{\sqrt{6}} (|010111\rangle + |101011\rangle + |110101\rangle \\
&\quad + |111010\rangle + |011101\rangle + |101110\rangle) \\
|T_6\rangle_6 &= \frac{1}{\sqrt{6}} \left( |010111\rangle + e^{i\pi/3}|101011\rangle + e^{i2\pi/3}|110101\rangle \right. \\
&\quad \left. + e^{i\pi}|111010\rangle + e^{i4\pi/3}|011101\rangle + e^{i5\pi/3}|101110\rangle \right) \\
|T_6^*\rangle_6 &= (|T_6\rangle_6)^* \\
|T_6'\rangle_6 &= \frac{1}{\sqrt{6}} \left( |010111\rangle + e^{i2\pi/3}|101011\rangle + e^{i4\pi/3}|110101\rangle \right. \\
&\quad \left. + |111010\rangle + e^{i2\pi/3}|011101\rangle + e^{i4\pi/3}|101110\rangle \right) \\
|T_6''\rangle_6 &= \frac{1}{\sqrt{6}} (|010111\rangle - |101011\rangle + |110101\rangle \\
&\quad - |111010\rangle + |011101\rangle - |101110\rangle) \\
|W_7\rangle_6 &= \frac{1}{\sqrt{6}} (|111000\rangle + |011000\rangle + |001110\rangle \\
&\quad + |000111\rangle + |100011\rangle + |110001\rangle) \\
|T_7\rangle_6 &= \frac{1}{\sqrt{6}} \left( |111000\rangle + e^{i\pi/3}|011100\rangle + e^{i2\pi/3}|001110\rangle \right. \\
&\quad \left. + e^{i\pi}|000111\rangle + e^{i4\pi/3}|100011\rangle + e^{i5\pi/3}|110001\rangle \right) \\
|T_7^*\rangle_6 &= (|T_7\rangle_6)^* \\
|T_7'\rangle_6 &= \frac{1}{\sqrt{6}} \left( |111000\rangle + e^{i2\pi/3}|011100\rangle + e^{i4\pi/3}|001110\rangle \right. \\
&\quad \left. + |000111\rangle + e^{i2\pi/3}|100011\rangle + e^{i4\pi/3}|110001\rangle \right) \\
|T_7''\rangle_6 &= \frac{1}{\sqrt{6}} (|111000\rangle - |011100\rangle + |001110\rangle \\
&\quad - |000111\rangle + |100011\rangle - |110001\rangle) \\
|W_8\rangle_6 &= \frac{1}{\sqrt{6}} (|101100\rangle + |010110\rangle + |001011\rangle \\
&\quad + |100101\rangle + |110010\rangle + |011001\rangle) \\
|T_8\rangle_6 &= \frac{1}{\sqrt{6}} \left( |101100\rangle + e^{i\pi/3}|010110\rangle + e^{i2\pi/3}|001011\rangle \right. \\
&\quad \left. + e^{i\pi}|100101\rangle + e^{i4\pi/3}|110010\rangle + e^{i5\pi/3}|011001\rangle \right) \\
|T_8^*\rangle_6 &= (|T_8\rangle_6)^* \\
|T_8'\rangle_6 &= \frac{1}{\sqrt{6}} \left( |101100\rangle + e^{i2\pi/3}|010110\rangle + e^{i4\pi/3}|001011\rangle \right. \\
&\quad \left. + |100101\rangle + e^{i2\pi/3}|110010\rangle + e^{i4\pi/3}|011001\rangle \right) \\
|T_8''\rangle_6 &= \frac{1}{\sqrt{6}} (|101100\rangle - |010110\rangle + |001011\rangle \\
&\quad - |100101\rangle + |110010\rangle - |011001\rangle) \\
|W_9\rangle_6 &= \frac{1}{\sqrt{6}} (|110100\rangle + |011010\rangle + |001101\rangle \\
&\quad + |100110\rangle + |010011\rangle + |101001\rangle) \\
|T_9\rangle_6 &= \frac{1}{\sqrt{6}} \left( |110100\rangle + e^{i\pi/3}|011010\rangle + e^{i2\pi/3}|001101\rangle \right. \\
&\quad \left. + e^{i\pi}|100110\rangle + e^{i4\pi/3}|010011\rangle + e^{i5\pi/3}|101001\rangle \right) \\
|T_9^*\rangle_6 &= (|T_9\rangle_6)^* \\
|T_9'\rangle_6 &= \frac{1}{\sqrt{6}} \left( |110100\rangle + e^{i2\pi/3}|011010\rangle + e^{i4\pi/3}|001101\rangle \right. \\
&\quad \left. + |100110\rangle + e^{i2\pi/3}|010011\rangle + e^{i4\pi/3}|101001\rangle \right) \\
|T_9''\rangle_6 &= \frac{1}{\sqrt{6}} (|110100\rangle - |011010\rangle + |001101\rangle \\
&\quad - |100110\rangle + |010011\rangle - |101001\rangle) \\
|W_{10}\rangle_6 &= \frac{1}{\sqrt{3}} (|100100\rangle + |010010\rangle + |001001\rangle) \\
|T_{10}\rangle_6 &= \frac{1}{\sqrt{3}} \left( |100100\rangle + e^{i2\pi/3}|010010\rangle + e^{i4\pi/3}|001001\rangle \right) \\
|T_{10}^*\rangle_6 &= (|T_{10}\rangle_6)^* \\
|W_{11}\rangle_6 &= \frac{1}{\sqrt{3}} (|110110\rangle + |011011\rangle + |101101\rangle) \\
|T_{11}\rangle_6 &= \frac{1}{\sqrt{3}} \left( |011011\rangle + e^{i2\pi/3}|101101\rangle + e^{i4\pi/3}|110110\rangle \right) \\
|T_{11}^*\rangle_6 &= (|T_{11}\rangle_6)^* \\
|GHZ_1'\rangle_6 &= \frac{1}{\sqrt{2}} (|101010\rangle + |101010\rangle) \\
|GHZ_2'\rangle_6 &= \frac{1}{\sqrt{2}} (|101010\rangle - |101010\rangle). \tag{13}
\end{aligned}$$

It is not difficult to verify, for instance,

$$\begin{aligned}\hat{T}|T_1\rangle_6 &= e^{-i\pi/3}|T_1\rangle_6 \\ \hat{T}|T'_1\rangle_6 &= e^{-i2\pi/3}|T'_1\rangle_6 \\ \hat{T}|T''_1\rangle_6 &= -|T''_1\rangle_6.\end{aligned}\quad (14)$$

Interestingly there are two entangled state of 3-period, which are double replications of 3-qubit case. It is not strange since the values of  $c$  corresponds to the characters of point group  $C_6$ , which consists of two  $C_3$  subgroups, as shown in Fig.7.

By LOCC, there are 8 classes determined by the periodicity and cyclic units,

$$\begin{aligned}&\left\{|GHZ_{1(2)}\rangle_6, |GHZ'_{1(2)}\rangle_6\right\}, \\&\left\{|W_{10(11)}\rangle_6, |T_{10(11)}\rangle_6, |T_{10(11)}^*\rangle_6\right\}, \\&\left\{|W_{1(2)}\rangle_6, |T_{1(2)}\rangle_6, |T_{1(2)}^*\rangle_6, |T'_{1(2)}\rangle_6, |T_{1(2)}'^*\rangle_6, |T''_{1(2)}\rangle_6\right\}, \\&\left\{|W_{3(4)}\rangle_6, |T_{3(4)}\rangle_6, |T_{3(4)}^*\rangle_6, |T'_{3(4)}\rangle_6, |T_{3(4)}'^*\rangle_6, |T''_{3(4)}\rangle_6\right\}, \\&\left\{|W_{5(6)}\rangle_6, |T_{5(6)}\rangle_6, |T_{5(6)}^*\rangle_6, |T'_{5(6)}\rangle_6, |T_{5(6)}'^*\rangle_6, |T''_{5(6)}\rangle_6\right\} \\&\left\{|W_7\rangle_6, |T_7\rangle_6, |T_7^*\rangle_6, |T_7'\rangle_6, |T_7'^*\rangle_6, |T_7''\rangle_6\right\} \\&\left\{|W_8\rangle_6, |T_8\rangle_6, |T_8^*\rangle_6, |T_8'\rangle_6, |T_8'^*\rangle_6, |T_8''\rangle_6\right\} \\&\left\{|W_9\rangle_6, |T_9\rangle_6, |T_9^*\rangle_6, |T_9'\rangle_6, |T_9'^*\rangle_6, |T_9''\rangle_6\right\}.\end{aligned}\quad (15)$$

The first class can be considered as 2-period, the second class as 3-period. The last 6 classes are all 6-period, distinguished by cyclic units.

### Symmetric basis as a eigenvector set of local Hamiltonian

Consider the ferromagnetic Hamiltonian

$$H_F^N = -\sum_{n=1}^N \sigma_n^z \sigma_{n+1}^z, \quad (16)$$

with boundary condition  $\sigma_{N+1}^z = \sigma_1^z$ .

*3-qubit case* There are two degenerate ground states,  $|GHZ_1\rangle_3$  and  $|GHZ'_1\rangle_3$ , with energy  $E_0 = -3$ . When one spin or two spins is flipped, one obtain the degenerate first excited states,  $|W_{1(2)}\rangle_3, |T_{1(2)}\rangle_3$  and  $|T_{1(2)}^*\rangle_3$ , with energy  $E_1 = 1$

It is obviously that the two classes of symmetric basis of 3-qubit are separated by a energy gap  $\Delta E = 4$ . Thus the conversion between the two classes has to close the gap, i.e., a phase transition.

*4-qubit case* The two degenerate ground states are  $|GHZ_1\rangle_4$  and  $|GHZ_2\rangle_4$ , with energy  $E_0 = -4$ . There are two different situation for first excited states; The first is that only one spin is flipped,  $|W_{1(2)}\rangle_4, |T_{1(2)}\rangle_4, |T_{1(2)}^*\rangle_4$  and  $|T'_{1(2)}\rangle_4$ . The second is that two nearest neighbored spins are flipped simultaneously,  $|W_3\rangle_4, |T_3\rangle_4, |T_3^*\rangle_4$  and

$|T'_3\rangle_4$ . The two distinct features can be differentiated by introducing the next nearest neighbored perturbation  $H^I = -\lambda(\sigma_1^z \sigma_3^z + \sigma_2^z \sigma_4^z)$  with  $\lambda \ll 1$ . Then one has the energy  $E'_1 = 0$  for the first case,  $E''_1 = 2\lambda$  for the second case.

The highest levels are  $|GHZ'_1\rangle_4$  and  $|GHZ'_2\rangle_4$  with energy  $E_2 = 4$ . Interestingly they also are the degenerate ground states of  $H_{AF}^4 = -H_F^4$ , which has local unitary equivalence  $H_{AF}^4 = (\sigma_1^x \otimes I_2 \otimes \sigma_3^x \otimes I_4) H_F^4 (\sigma_1^x \otimes I_2 \otimes \sigma_3^x \otimes I_4)$ . Consequently  $|GHZ'_{1(2)}\rangle_4$  is LOCC equivalent to  $|GHZ_{1(2)}\rangle_4$ .

*5-qubit*  $|GHZ_1\rangle_5$  and  $|GHZ_2\rangle_5$  are still the ground states of  $H_F^5$ . Similar to 4-qubit case, the first excited state have two distinct structures,  $\left\{|W_{1(2)}\rangle_5, |T_{1(2)}\rangle_5, |T_{1(2)}^*\rangle_5, |T'_{1(2)}\rangle_5\right\}$  and  $\left\{|W_{3(4)}\rangle_5, |T_{3(4)}\rangle_5, |T_{3(4)}^*\rangle_5, |T'_{3(4)}\rangle_5\right\}$ . In addition, one can also introduce the next nearest neighbored interaction  $H^I = -\lambda \sum_{n=1}^5 \sigma_n^z \sigma_{n+2}^z$  in order to differentiate them. Then one has total energy  $E'_1 = -1 - \lambda$  for the former and  $E'_1 = -1 + 3\lambda$  for the latter. Finally the class  $\left\{|W_{5(6)}\rangle_5, |T_{5(6)}\rangle_5, |T_{5(6)}^*\rangle_5, |T'_{5(6)}\rangle_5\right\}$  composes the highest level.

*6-qubit case* Except of the degenerate ground states  $|GHZ_1\rangle_6$  and  $|GHZ_2\rangle_6$ , this case is complex.

The first excited state with  $E_1 = -2$  have three distinct structures,  $\left\{|W_{1(2)}\rangle_6, |T_{1(2)}\rangle_6, |T_{1(2)}^*\rangle_6, |T'_{1(2)}\rangle_6, |T_{1(2)}'^*\rangle_6, |T''_{1(2)}\rangle_6\right\}$ ,  $\left\{|W_{3(4)}\rangle_6, |T_{3(4)}\rangle_6, |T_{3(4)}^*\rangle_6, |T'_{3(4)}\rangle_6, |T_{3(4)}'^*\rangle_6, |T''_{3(4)}\rangle_6\right\}$ , and  $\left\{|W_7\rangle_6, |T_7\rangle_6, |T_7^*\rangle_6, |T_7'\rangle_6, |T_7'^*\rangle_6, |T_7''\rangle_6\right\}$ . By introducing the next nearest interaction  $H^I = -\lambda \sum_{n=1}^6 \sigma_n^z \sigma_{n+2}^z$ , the energy becomes  $E'_1 = -2 - 2\lambda$  for the first case and  $E''_1 = -2 + 2\lambda$  for the other two cases. The one has to introduce the next next neighbored interaction in order to differentiate the latter two cases.

The second excited states  $E_2 = 2$  include four distinct classes,  $\left\{|W_{5(6)}\rangle_6, |T_{5(6)}\rangle_6, |T_{5(6)}^*\rangle_6, |T'_{5(6)}\rangle_6, |T_{5(6)}'^*\rangle_6, |T''_{5(6)}\rangle_6\right\}$ ,  $\left\{|W_8\rangle_6, |T_8\rangle_6, |T_8^*\rangle_6, |T_8'\rangle_6, |T_8'^*\rangle_6, |T_8''\rangle_6\right\}$ ,  $\left\{|W_9\rangle_6, |T_9\rangle_6, |T_9^*\rangle_6, |T_9'\rangle_6, |T_9'^*\rangle_6, |T_9''\rangle_6\right\}$ , and  $\left\{|W_{10(11)}\rangle_6, |T_{10(11)}\rangle_6, |T_{10(11)}^*\rangle_6\right\}$ . By introducing the next nearest interaction, one can only differentiate the first from the other. Furthermore by introducing the next next neighbored interaction, the last can be singled out. As for the remained two cases, there seems no efficient interaction to differentiate them.

The highest level corresponds to  $|GHZ'_{1(2)}\rangle_6$  with  $E_3 = 6$ . Similar as 4-qubit case, they also the ground states of  $H_{AF}^6 = -H_F^6$ , of which equivalence is  $H_{AF}^6 = (\sigma_1^x \otimes I_2 \otimes \sigma_3^x \otimes I_4 \otimes \sigma_5^x \otimes I_6) H_F^6 (\sigma_1^x \otimes I_2 \otimes \sigma_3^x \otimes I_4 \otimes \sigma_5^x \otimes I_6)$ . Thus  $|GHZ'_{1(2)}\rangle_6$  are LOCC equivalent to  $|GHZ_{1(2)}\rangle_6$ . However this relation cannot be generalized to the other excited states since this transformation has special

symmetric structure.